Applied Physics Letters

Vertical two-dimensional layered conjugated porous organic network structures of poly-benzimidazobenzophenanthroline (BBL): A first-principles study

Cite as: Appl. Phys. Lett. **117**, 233101 (2020); https://doi.org/10.1063/5.0035132
Submitted: 29 October 2020 . Accepted: 25 November 2020 . Published Online: 08 December 2020

A. Bafekry, M. M. Fadlallah, C. Nguyen, and D. Gogova

Applied Physics Letters ARTICLE scitation.org/journal/apl

Vertical two-dimensional layered conjugated porous organic network structures of poly-benzimidazobenzophenanthroline (BBL): A first-principles study

Cite as: Appl. Phys. Lett. **117**, 233101 (2020); doi: 10.1063/5.0035132
Submitted: 29 October 2020 · Accepted: 25 November 2020 ·
Published Online: 8 December 2020

A. Bafekry,[1,a] M. M. Fadlallah,[2,b] C. Nguyen,[3] and D. Gogova[4]

AFFILIATIONS

[1]Department of Physics, University of Guilan, 41335-1914 Rasht, Iran
[2]Department of Physics, Faculty of Science, Benha University, 13518 Benha, Egypt
[3]Department of Materials Science and Engineering, Le Quy Don Technical University, Ha Noi 100000, Vietnam
[4]Department of Physics, University of Oslo, P.O. Box 1048, Blindern, Oslo, Norway

[a]Author to whom correspondence should be addressed: bafekry.asad@gmail.com
[b]mohamed.fadlallah@fsc.bu.edu.eg

ABSTRACT

Very recently, the 2D form of poly-benzimidazobenzophenanthroline (BBL) structures has been successfully fabricated [Noh *et al.*, Nat. Commun. **369**, 670 (2020)]. Motivated by these exciting experimental results on 2D layered BBL structures, herein we perform density functional theory-based first-principles calculations in order to gain insight into the structural, electronic, and optical properties of the BBL monolayer and bilayer honeycomb crystal structures (planar and vertical). Our computational structural optimization reveals that the BBL monolayer crystallizes in a puckered, anisotropic hexagonal structure, while the BBL bilayer is composed of covalently bonded shifted one with respect to the other BBL layers. Two terminations with hydrogen and fluorine atoms are considered for the BBL bilayer, namely, H-BBL and F-BBL, respectively. The direct bandgaps of H-BBL_s and F-BBL_s are $\sim$ 1 eV and $\sim$ 1.2 eV. The top of the valence band and the bottom of the conduction band are flat due to the localized carbon states. The BBL monolayer and bilayer can absorb a wide range of visible light. The calculated refractive index of the BBL monolayer is $\sim$ 1, i.e., it is smaller than the refractive index of the common natural or synthetic polymers.

The successful discovery of graphene by Geim and colleagues[1] and its unusual physical properties have motivated the scientific community in the search for novel layered materials with promising characteristics for designing high-performance nanodevices. In addition to the search for novel two-dimensional graphene-like materials, such as transition metal dichalcogenides[2–4] and phosphorene,[5,6] the scientific community has also focused on planar 2D porous organic networks,[7–12] metal and covalent organic frameworks,[13,14] porous coordination polymers,[15] and porous cage-like structures.[16] These 2D organic networks can be considered as promising candidates for high-performance applications.[17–19] Unfortunately, most of these organic networks exhibit poor stability at room temperature, which hinders their practical applications. Therefore, finding a way to improve the stability and the search for new organic networks with better properties are very challenging tasks nowadays.

The poly-benzimidazobenzophenanthroline layer (BBL) is an 1D planar organic network, which contains multiple strands of fused aromatic rings.[20,21] The BBL was experimentally synthesized a long time ago.[22] Furthermore, several 1D BBL_s were created employing different strategies.[23,24] It is interesting that the conjugated ladder BBL proposed by Van Deusen[22] exhibits excellent chemical and thermal stability due to the expanded π-conjugated systems. Owing to the extraordinary properties, the ladder-type BBL_s are suitable for the design of new organic nanodevices, such as field-effect transistors,[25–27] as well as for photovoltaic solar cells.[28]

Very recently, a new class of organic networks, namely, a 2D layered benzimidazobenzophenanthroline layer has been developed by

reacting triptycene hexamine with naphthalenetetracarboxylic dianhydride.[29] It has been demonstrated that the thermal, chemical, and mechanical stability increase as the extended π-conjugated systems increase.[20,30] The conjugated 2D-BBL$_s$ are expected to offer significant advantages over their 1D linear analogues such as larger specific surface area, microporosity, and functionality.[29] The bilayer BBL structure has two configurations: (1) parallel BBL (the second BBL layer is parallel to the stacking direction) and (2) vertical BBL (the second BBL layer is perpendicular to the stacking direction).[29] Also, two different terminations with hydrogen and fluorine atoms H-terminated BBL$_s$ (H-BBL$_s$) and F-terminated BBL$_s$ (F-BBL$_s$) are considered in this study.

Recently, the planar 2D layered BBL has been used to remove toxic ions, a property with huge application potential.[31] Therefore, motivated by the recent experimental realization of the 2D BBL structures, in this study we investigate the structural, electronic, and optical properties of monolayer and bilayer forms of the 2D BBL polymers by theoretical approaches. Our computational results reveal that the BBL monolayer crystallizes in a puckered, anisotropic hexagonal structure, while the BBL bilayer is composed of covalently bonded shifted one with respect to the other two BBL layers. The bandgaps of the H-BBL$_s$ and F-BBL$_s$ have been determined to be ∼1 eV and ∼1.2 eV, respectively. The BBL monolayer and bilayer can absorb a wide range of visible light. The calculated refractive index of the BBL monolayer is ∼1, which is smaller than the refractive indexes of the common polymers with natural or synthetic origin.

All calculations were performed using the SIESTA code,[32] based on the density functional theory. The wave functions were expanded by the linear combination of atomic orbitals (LCAOs). The generalized gradient approximation in the scheme of Perdew–Burke–Ernzerhof was employed as the exchange-correlation functional.[33] The double zeta basis sets and norm-conserving Troullier–Martins pseudopotentials[34] for core electrons were used. The cutoff energy is 250 eV and the geometries were fully relaxed until the force acting on each atom is less than 0.04 eV/Å and the total energy converges until 1.0 meV/atom. The k-points for sampling over the Brillouin zone (BZ) integration were generated employing the Monkhorst-Pack scheme and were determined using 23 × 23 × 1 for the primitive unit cell. For the supercell including one BBL monolayer (100 atoms) and the planar and vertical BBL bilayers (256 atoms), the 5 × 5 × 1 k-mesh was used. We set the vacuum region in the z-direction that separates the successive BBL layer and bilayer at 20 Å to avoid interaction between adjacent layers. The DFT-D2 method is also applied to describe the weak interactions, existing in the BBL bilayer. Spin-polarized calculations were performed to check the presence of magnetic behavior. The computational results showed that the 2D BBL polymers are non-magnetic semiconductors in the ground state.

Figure 1(a) discloses the structure of the BBL monolayer in different views, while Fig. 2(a) illustrates the BBL (I) bilayer, where the two layers are in the same direction of stacking (AA stacking). Figure 2(b) shows the BBL (II) bilayer with stacking AB of the two layers. The calculated lattice constant of the monolayer is 29.97 Å, while the lattice constant of the both types of bilayers is 29.66 Å, as listed in Table I. The thickness of the BBL defined by the difference between the largest and smallest distances in the z-direction is determined as 4.39 Å for the monolayer and 7.73 Å for the bilayer. The nanopore diameter of the BBL monolayer and bilayer is ∼34.65 Å and the distance between the nearest two branches (L) in the BBL is calculated to be 17.52 Å for the monolayer and 17.41 Å for the bilayer [see Fig. 1(a), blue square]. The distance between the two layers in the BBL bilayer is 3.10 Å. All the optimized structure parameters and bond lengths between the atoms of the BBL monolayer and bilayer are elucidated in Table I.

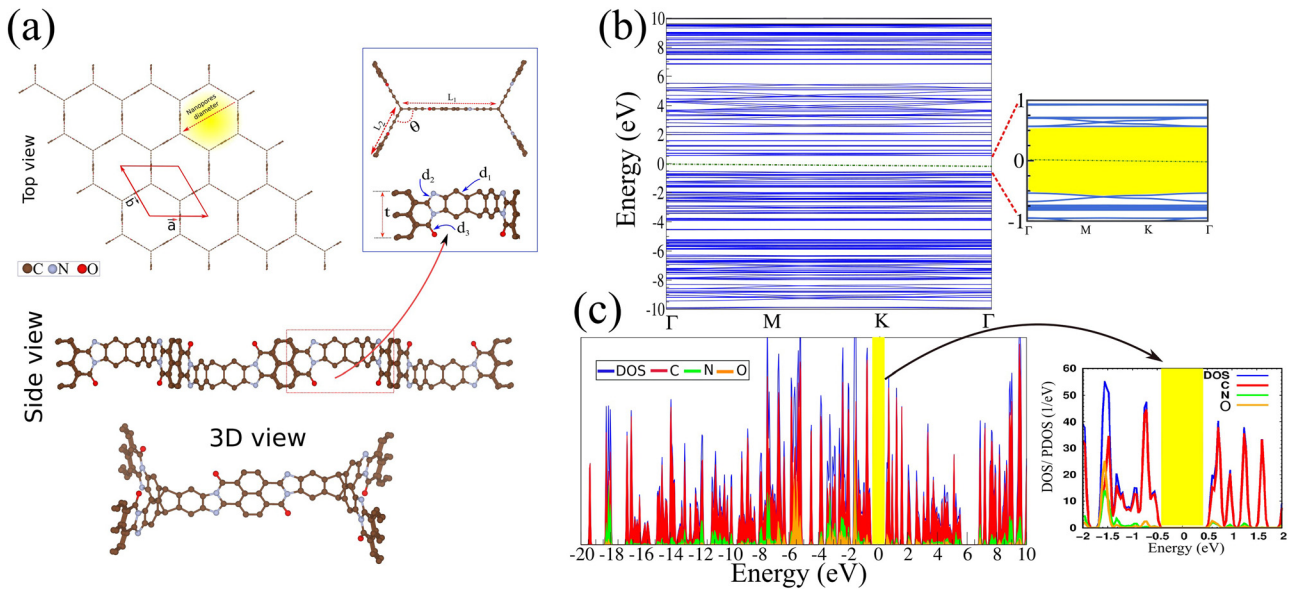

FIG. 1. (a) Different views of the BBL monolayer atomic structure with a primitive unit cell indicated by a red hexagonal. A schematic view of the BBL monolayer structure with the structural parameters is shown by the blue line square. (b) Electronic band structure of the BBL monolayer. Zoom of the band structure indicated in the left panel. (c) DOS/PDOS of the BBL-monolayer. Zoom of DOS/PDOS indicated in the left panel. The zero of energy is set to the Fermi level.

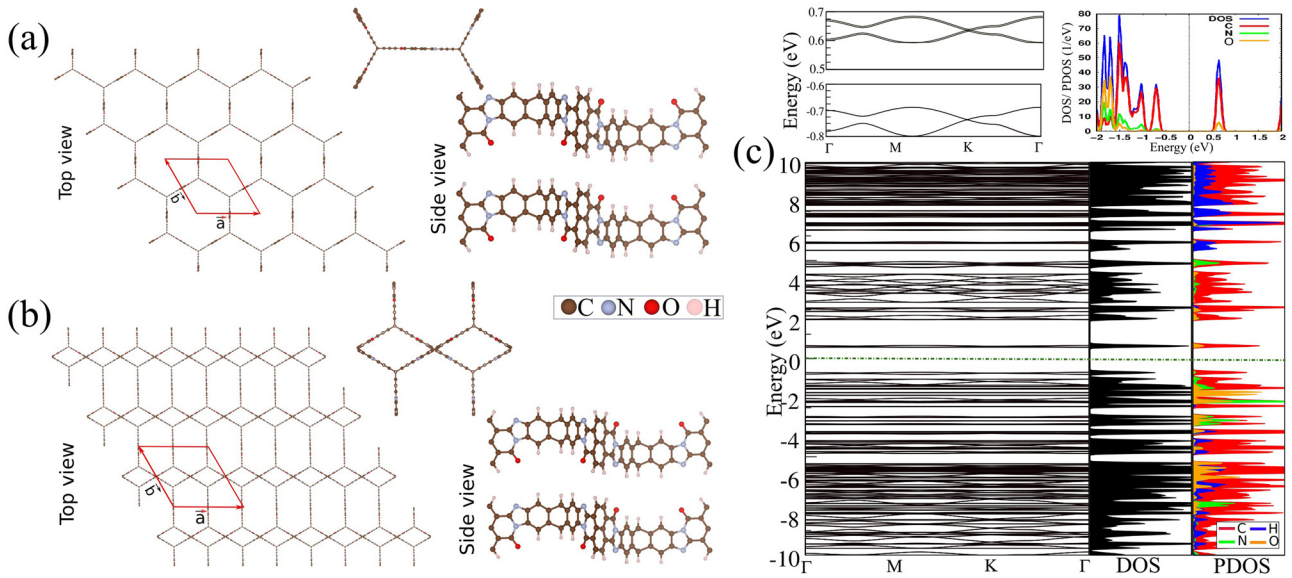

FIG. 2. Different views of the atomic structure of the H-BBL bilayer in the (a) planar AA-stacking (I) and (b) vertical AB-stacking (II) with the primitive unit cell indicated by a red hexagonal. Schematic view of the BBL monolayer structure with structural parameters is shown in the right panel. (c) Electronic band structure and DOS/PDOS of the H-BBL bilayer (I). Zoom of the band structure and DOS/PDOS indicated in the top panel. The zero of energy is set to the Fermi level.

The cohesive energy E_{coh} for the monolayer and bilayer is then given by

$$E_{coh} = \frac{n_C E_C + n_N E_N + n_O E_O + -E_{tot}}{n_{tot}}, \quad (1)$$

$$E_{coh} = \frac{n_C E_C + n_N E_N + n_O E_O + n_{H(F)} E_{H(F)} - E_{tot}}{n_{tot}}, \quad (2)$$

respectively, where n_x and E_x are the number of x atoms and the energy of x atoms, $x = C, N, O, H, F$, respectively. n_{tot} and E_{tot} represent the total number of atoms and total energy, respectively. The energy of atoms is calculated using the energy of the x^2 molecule, $E_x = E(x^2)/2$. The cohesive energy is found to be −7.72 eV/atom for the monolayer, −7.44 (−8.35) eV/atom for the H-(F-)BBL planar bilayer, and −7.33 (−8.12) eV/atom for the H-(F-)BBL vertical bilayer. The negative sign of the energy confirms the stability of the BBL structures. The cohesive energy of F-terminated structures is more stable than that of the corresponding H-terminated structures due the higher electronegativity of F as compared to H. In addition, one can find that the cohesive energies are comparable to those of other systems, including graphene (−7.9 eV/atom)[35] and diamond (−7.73 eV/atom),[36] implying that these 2D BBL systems are structurally stable.

The density of states (DOS), projected DOS (PDOS), and band structures of the BBL monolayer are exhibited in Figs. 1(b) and 1(c). The calculated direct bandgap value is 0.95 eV, and the C states dominate in the considered energy range. The O and N states have a significant contribution at −1.6 eV and little contributions above −1.6 eV as well as in the conduction band. The band structures show the flat bands at the top of the valence band and the bottom of conduction bands due to the localized states of C atoms at the band edges.

Figure 2(c) shows the DOS/PDOS and band structure of the planar H-BBL bilayer. The effect of interaction between the two layers has significant changes in the DOS as compared to the DOS of the BBL monolayer. The band structure is slightly shifted toward the low

TABLE I. The structural and electronic parameters of the BBL monolayer and BBL bilayer shown in Fig. 1. The corresponding structural and electronic parameters including the lattice constant (a); the bond length between C–C, C–N, C–O, and C–H (F) atoms (d_1, d_2, d_3, and d_4); the bond angles between C lines atom atoms (θ); the thickness of the BBL defined by the difference between the largest and smallest z coordinates of atoms (t); the distance between atoms ($L_{1,2}$); the distance layer (h); the nanopore diameter (D); the cohesive energy per atom, (E_{coh}); the electronic state (ES) specified as a semiconductor (SC); and the bandgap (E_g).

	a (Å)	d_1 (Å)	d_2 (Å)	d_3 (Å)	d_4 (Å)	(t) (Å)	(h) (Å)	$L_{1,2}$ (Å)	D (Å)	θ_1 (°)	E_{coh} (eV/atom)	E_g (eV)
BBL monolayer	29.97	1.41	1.42	1.22	…	4.89	…	17.52, 8.18	34.64	104	−7.72	SC (0.95)
H-BBL bilayer (I)	29.66	1.42	1.40	1.23	1.08	7.73	3.11	17.41, 8.17	34.60	105	−7.44	SC (1.00)
H-BBL bilayer (II)	29.66	1.42	1.40	1.23	1.08	7.73	3.12	17.41, 8.17	34.66	105	−7.33	SC (1.02)
F-BBL bilayer (I)	29.66	1.41	1.36	1.22	1.33	7.23	3.10	17.44, 9.97	34.62	105	−8.53	SC (1.18)
F-BBL bilayer (II)	29.66	1.41	1.36	1.22	1.33	7.22	3.11	17.47, 10.16	34.62	105	−8.12	SC (1.20)

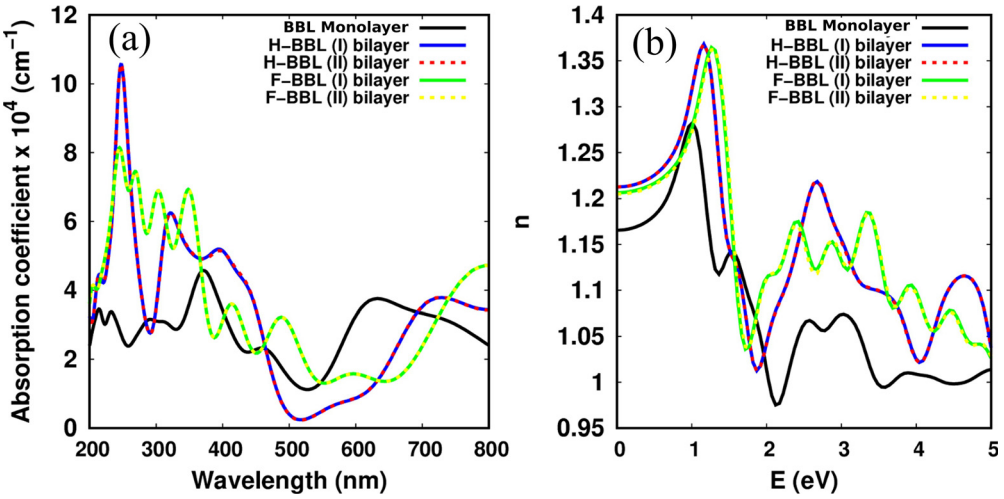

FIG. 3. Numerically calculated spectral dependencies of the absorption coefficient (a) and the refractive index (b) of the BBL monolayer and bilayer.

energy. The C states dominate in the energy range from −1.6 to −0.6 eV and at 0.6 eV, while the O states dominate below −1.6 with a certain contribution of the H states. Thus, a direct bandgap becomes 1.00 eV, which is slightly larger than the bandgap of the BBL monolayer. There are no states in the energy range of 0.6–1.9 eV. For the vertical H-BBL bilayer in the AA-stacking, the behavior of the electronic structure is very similar to the planar case (see supplementary material, Fig. S1). The bandgap is 1.02 eV, which is slightly larger than the corresponding values of the monolayer and the planar bilayer. For the F-BBL bilayer, we also found that the electronic structures for planar and vertical structures are very similar (see supplementary material, Fig. S2). The direct bandgaps of the planar and vertical F-BBLs are 1.18 eV and 1.20 eV, respectively.

The absorption spectra ($\alpha(\omega)$) and refractive index ($n(\omega)$) are calculated using

$$\alpha(\omega) = \sqrt{2}\omega\sqrt{\sqrt{\varepsilon_1^2(\omega) + \varepsilon_2^2(\omega)} - \varepsilon_1(\omega)} \tag{3}$$

and

$$n(\omega) = \frac{1}{\sqrt{2}}\left(\sqrt{\varepsilon_1^2(\omega) + \varepsilon_2^2} + \varepsilon_1(\omega)\right)^{1/2}, \tag{4}$$

where $\varepsilon_1(\omega)$ and $\varepsilon_2(\omega)$ are the real and imaginary parts of the dielectric function at angular frequency ω, respectively. The transmission matrix between the valence band ψ_k^v and conduction band ψ_k^c is calculated to evaluate $\varepsilon_2(\omega)$ by

$$\varepsilon_2(\omega) = \frac{(2\pi e)^2}{(m\omega)^2 V}\sum_{k,i}\langle\psi_k^v|p_i|\psi_k^c\rangle\delta(E_{\psi_k^c} - E_{\psi_k^v} - \hbar\omega), \tag{5}$$

and the Kramers–Kronig relation is used to obtain

$$\varepsilon_1(\omega) = \frac{2}{\pi}P\int d\omega' \frac{\varepsilon_2(\omega')}{\omega' - \omega}, \tag{6}$$

where e, m, V, and p are the charge, mass of the electron, volume of the supercell, and momentum operator. $E_{\psi_k^v}$, $E_{\psi_k^c}$, and $\hbar\omega$ are the occupied, unoccupied, and incident light energies, respectively. P in Eq. (5) indicates that the integral is calculated by the Cauchy's principal value. Figure 3(a) shows the absorption coefficient of the BBL monolayer. Several peaks emerge at 220, 300, 380, 460, and 650 nm. The highest peak appears at 380 nm, and the widest peak occurs at 650 nm. The BBL can absorb the UV and a wide range of visible light. For bilayer (I), the absorption peaks have shifted toward higher wavelengths and they appear at 250 nm, 320 nm, 400 nm, and 720 nm. The H-(F-)BBL bilayer (I) can absorb longer wavelengths as compared to the monolayer. The H-(F-)BBL bilayer (II) absorption spectra are very similar to the corresponding H-(F-)BBL bilayer (I) ones due to the similarity of their electronic structures. The absorbed light by the H-(F-)BBL bilayer is larger than the corresponding one by the monolayer in the wavelength range from 200 to 480 nm and above 750 nm due to the larger thickness of the bilayer.

Figure 3(b) depicts the refractive index dispersion of the BBL monolayer. The first distinct peak of the BBL monolayer appears at 1.0 eV (1240 nm) and of the bilayers at ∼1.2 eV (1033 nm). The refractive index of the BBL monolayer is 0.98 and that of the BBL bilayer is 1.1. These values are close to the refractive index value of air and, meanwhile, are lower than those of the common polymers[37] at 2.1 eV (589 nm). The refractive index of the BBL bilayer is larger than the corresponding one of the monolayer.

First-principles calculations have been used to investigate the structural, electronic, and optical properties of 2D BBL polymers. We found out that the structure parameters of the BBL bilayers for AA and AB stackings are the same. Also, there is no change in the electronic and optical properties for AA and AB stackings. The bandgap of the BBL monolayer is 0.95 eV, which is very similar to the BBL bilayer bandgap of ∼1 eV. The ability of the BBL bilayer to absorb light is larger than that of the BBL monolayer. Our findings show that the refractive index of the BBL monolayer and bilayer is ∼1.

See the supplementary material for the complete electronic structure with the corresponding density of states of the studied F-terminated BBL bilayer.

This work was funded by the Research Council of Norway SALIENT Project (No. 239895/F20) and the Vietnam National Foundation for Science and Technology Development (NAFOSTED) under Grant No. 103.01-2019.05. Also, this work was funded by the Research Council of Norway (RCN) SALIENT Project (No. 239895/F20) and the Vietnam National Foundation for Science and Technology Development (NAFOSTED) under Grant No. 103.01-2019.05.

DATA AVAILABILITY

The data that support the findings of this study are available from the corresponding author upon request.

REFERENCES

[1]K. S. Novoselov, A. K. Geim, S. V. Morozov, D. Jiang, Y. Zhang, S. V. Dubonos, I. V. Grigorieva, and A. A. Firsov, Science **306**, 666 (2004).
[2]S. Manzeli, D. Ovchinnikov, D. Pasquier, O. V. Yazyev, and A. Kis, Nat. Rev. Mater. **2**, 17033 (2017).
[3]Q. H. Wang, K. Kalantar-Zadeh, A. Kis, J. N. Coleman, and M. S. Strano, Nat. Nanotechnol. **7**, 699 (2012).
[4]K. F. Mak and J. Shan, Nat. Photonics **10**, 216 (2016).
[5]E. S. Reich, Nature **506**, 19 (2014).
[6]A. Carvalho, M. Wang, X. Zhu, A. S. Rodin, H. Su, and A. H. C. Neto, Nat. Rev. Mater. **1**, 16061 (2016).
[7]S. Das, P. Heasman, T. Ben, and S. Qiu, Chem. Rev. **117**, 1515 (2017).
[8]A. Bafekry, S. F. Shayesteh, and F. M. Peeters, J. Appl. Phys. **126**, 215104 (2019).
[9]A. Bafekry, C. Stampfl, B. Akgenc, B. Mortazavi, M. Ghergherehchi, and C. V. Nguyen, Phys. Chem. Chem. Phys. **22**, 6418 (2020).
[10]A. G. Slater and A. I. Cooper, Science **348**, aaa8075 (2015).
[11]A. Bafekry, M. Yagmurcukardes, M. Shahrokhi, and M. Ghergherehchi, Carbon **168**, 220 (2020).
[12]A. Bafekry and C. Stampfl, Phys. Rev. B **102**, 195411 (2020).
[13]H. Furukawa, K. E. Cordova, M. O'Keeffe, and O. M. Yaghi, Science **341**, 1230444 (2013).
[14]A. P. Cote, A. I. Benin, N. W. Ockwig, M. O'Keeffe, A. J. Matzger, and O. M. Yaghi, Science **310**, 1166 (2005).
[15]S. Kitagawa, R. Kitaura, and S.-I. Noro, Ang. Chem. Inter. **43**, 2334 (2004).
[16]A. I. Hasell and T. Cooper, Nat. Rev. Mater. **1**, 16053 (2016).
[17]Y. Zhang and S. N. Riduan, Chem. Soc. Rev. **41**, 2083 (2012).
[18]J. Mahmood, E. K. Lee, M. Jung, D. Shin, I.-Y. Jeon, S.-M. Jung, H.-J. Choi, J.-M. Seo, S.-Y. Bae, S.-D. Sohn *et al.*, Nat. Commun. **6**, 6486 (2015).
[19]H. Furukawa, O. M. Yaghi, and J. Ame, Chem. Soc. **131**, 8875 (2009).
[20]U. Scherf, J. Mater. Chem. **9**, 1853 (1999).
[21]J. Lee, A. J. Kalin, T. Yuan, M. Al-Hashimi, and L. Fang, Chem. Sci. **8**, 2503 (2017).
[22]R. L. Van Deusen, J. Polym. Sci., Part B **4**, 211 (1966).
[23]F. E. Arnold, J. Poly. Sci., Part B **7**, 749 (1969).
[24]J. K. Stille and M. E. Freeburger, J. Poly. Sci., Part B **5**, 989 (1967).
[25]A. Babel and S. A. Jenekhe, Adv. Mater. **14**, 371 (2002).
[26]H. Sun, M. Vagin, S. Wang, X. Crispin, R. Forchheimer, M. Berggren, and S. Fabiano, Adv. Mater. **30**, 1704916 (2018).
[27]F. S. Kim, E. Ahmed, S. Subramaniyan, and S. A. Jenekhe, Appl. Mater. Interfaces **2**, 2974 (2010).
[28]S. A. Jenekhe and S. Yi, Appl. Phys. Lett. **77**, 2635 (2000).
[29]H.-J. Noh, Y.-K. Im, S.-Y. Yu, J.-M. Seo, J. Mahmood, T. Yildirim, and J.-B. Baek, Nat. Commun. **11**, 2021 (2020).
[30]S. Wang, H. Sun, U. Ail, M. Vagin, P. O. Persson, J. W. Andreasen, W. Thiel, M. Berggren, X. Crispin, D. Fazzi, and S. Fabiano, Adv. Mater. **28**, 10764 (2016).
[31]S.-H. Shin, H.-J. Noh, Y.-H. Kim, Y.-K. Im, J. Mahmood, and J.-B. Baek, Polym. Chem. **10**, 4185 (2019).
[32]J. M. Soler, E. Artacho, J. D. Gale, A. Garcia, J. Junquera, P. Ordejon, and D. Sanchez-Portal, J. Phys.: Condens. Matter **14**, 2745 (2002).
[33]J. P. Perdew, K. Burke, and M. Ernzerhof, Phys. Rev. Lett. **77**, 3865 (1996).
[34]N. Troullier and J. L. Martins, Phys. Rev. B **43**, 1993 (1991).
[35]P. Koskinen, S. Malola, and H. Hakkinen, Phys. Rev. Lett. **101**, 115502 (2008).
[36]V. Ivanovskaya, A. Zobelli, D. Teillet-Billy, N. Rougeau, V. Sidis, P. Briddon, and T. Euro, Phys. J. B **76**, 481 (2010).
[37]J.-G. Liu and M. Ueda, J. Mater. Chem. **19**, 8907 (2009).